



## LJMU Research Online

**Chen, X, Opoz, TT and Oluwajobi, A**

**Analysis of grinding surface creation by single grit approach**

<http://researchonline.ljmu.ac.uk/id/eprint/7083/>

### Article

**Citation** (please note it is advisable to refer to the publisher's version if you intend to cite from this work)

**Chen, X, Opoz, TT and Oluwajobi, A (2017) Analysis of grinding surface creation by single grit approach. Journal of Manufacturing Science and Engineering, 139 (12). ISSN 1528-8935**

LJMU has developed **LJMU Research Online** for users to access the research output of the University more effectively. Copyright © and Moral Rights for the papers on this site are retained by the individual authors and/or other copyright owners. Users may download and/or print one copy of any article(s) in LJMU Research Online to facilitate their private study or for non-commercial research. You may not engage in further distribution of the material or use it for any profit-making activities or any commercial gain.

The version presented here may differ from the published version or from the version of the record. Please see the repository URL above for details on accessing the published version and note that access may require a subscription.

For more information please contact [researchonline@ljmu.ac.uk](mailto:researchonline@ljmu.ac.uk)

<http://researchonline.ljmu.ac.uk/>

## **Analysis of grinding surface creation by single grit approach**

X. Chen<sup>1</sup>, T. T. Öpöz<sup>1</sup> and A. Oluwajobi<sup>2</sup>

<sup>1</sup> General Engineering Research Institute, Liverpool John Moores University, Liverpool L3 3AF, UK

<sup>2</sup> Department of Mechanical Engineering, Faculty of Technology, Obafemi Awolowo University, P.M. B. 13: 220005, Ile-Ife, Nigeria

ASME ©

**Abstract:** This paper presents some new research findings in the investigation of single grit grinding in terms of surface creation. The investigation demonstrated that rubbing-ploughing-cutting hypothesis of grinding material removal mechanism is valid in both experiments and simulations. A finite element model (FEM) was developed to simulate the material deformation during the grit interacts with the workpiece. It was found that the cutting mechanism is the more effective in the first half of the scratch where the grit penetrates the workpiece. The ploughing is a prominent mechanism in the second half of the scratch where the grit is climbing up along the scratch path and uplifting the material at the front and the sides of it. This observation is very important to provide a greater insight into the difference between up-cut and down-cut grinding material removal mechanisms. Multi passes scratch simulations were performed to demonstrate the influence of ploughing on the ground surface formation. Moreover, by analysing the effects of grinding conditions, the shape of cutting edges and friction in grinding zone on the grinding surface formation, some useful relations between grinding performance and controllable parameters have been identified. It has demonstrated that ploughing has significant influences on ground surface formation and concluded that the influence of grit shape, friction and grinding kinetic condition should be considered together for the ploughing behaviour control, which could provide a good guidance for the improvement of grinding efficiency.

**Keywords:** surface creation; single grit grinding; scratching; finite element method.

# 1 Introduction

Grinding is one of the most commonly used material removal methods for a wide range of applications from ultra-precision surface creation to extremely high-speed material removal. Grinding is a very complicated process comparing to other machining processes that use geometrically defined cutting edges. Understand the material removal mechanism of grinding is a critical issue to define operational strategy for grinding process optimisation. Many researches have been undertaken in order to understand the material behaviours under different grinding conditions.

Due to the scale of grinding chip formation and the high speed of grinding, it is difficult to observe the material deformation and chip formation during grinding. The simulation of material processing using finite element method (FEM) is a convenient tool to illustrate the material behaviour during processing. With FEM, grinding process has been modelled using heat transfer modelling technique in which case grinding wheel has been modelled as moving heat source and using elasto-mechanical material characteristic where the grinding wheel has been modelled as mechanical surface pressure [1]. This type of model is called as macro-scale model which deal with the interaction between grinding wheel and workpiece [1, 2]. The other approach is modelling of single grain actions during grinding process and called as micro-scale model dealing with individual grain interaction with workpiece [1-6]. Micro-scale modelling of grinding is particularly suitable for simulation of grinding surface creation. However, it is still under developing stage due to the difficulty of FEM at the level of sub-micron level.

Micro-scale FEM model of grinding process was difficult because it requires high computational power. However, recently researchers have begun to investigate on micro-scale modelling and simulation of grinding process [1, 2, 7]. The grinding action of a single grain including rubbing, ploughing and cutting three phases was first put forth by Hahn [8]. The rubbing phase due to only elastic deformation is the shortest and generally results in negligible effect in terms of contribution to material removal. On the other hand, investigation and monitoring of the rubbing phase is the most

difficult task in grinding. Often, an acoustic emission (AE) system [9] is employed to detect and differentiate the different phases of material removal and their significances in grinding in terms of the contribution to the surface formation and actual chip removal. The ploughing phase involves both elastic and plastic deformation but no chip removal, which plays an important role in surface formation. Since the ploughing consumes a lot of energy without direct contribution to the material removal, it makes grinding specific energy become much higher than other cutting processes. The cutting phase where the actual chip formation takes place, involves the elastic and plastic deformation as well as the chip removal. This phase is considered as the most desired phase to utilise the energy for grinding to remove materials and create new surface. Detailed analysis of specific energy requirements for the each phase (rubbing, ploughing and chip formation) during the grinding and its relations to grinding parameters and abrasive grain wear behaviour is broadly covered in Malkin's book [10]. Fig. 1 illustrates a model of grinding chip formation mechanism in three phases. Upon increasing grit penetration depth through the rubbing and ploughing phase, when the grit reaches to the specific cutting depth, the chip removal initiates in the cutting phase [11, 12].

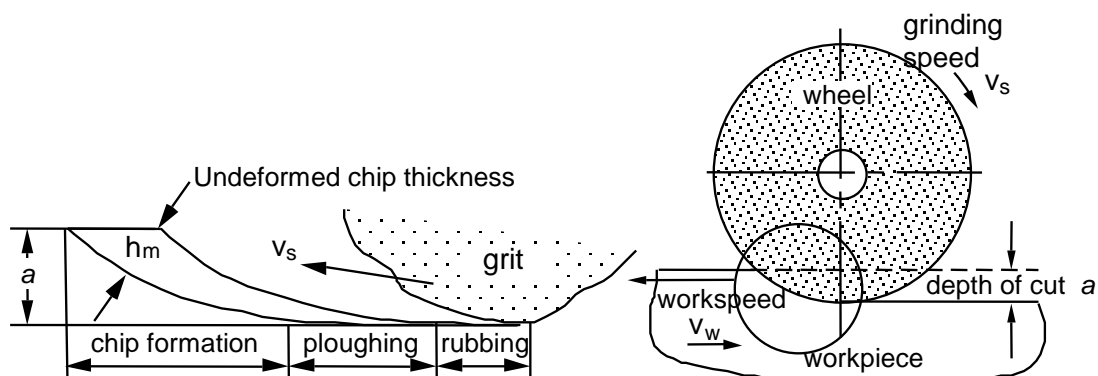


**Fig. 1** Grinding material removal three phases (rubbing, ploughing and cutting)

Single grain scratch tests have been conducted experimentally by many researchers in order to explore the single grain grinding mechanics and material removal mechanism at micro scale [12-20]. One of the earliest researches on single grain scratch over the workpiece was carried out by Takenaka

[13]. He found that the cutting action decreases with the decrease of depth of cut, however, the rate of the ploughing actions increases with decreasing depth of cut. Grain orientation during single grain scratching process is one of the influential factor which affect the material removal mechanism and cutting mechanics. Recent research shows that the orientation of the grain has significant effects on the energy requirement and material ploughing rate [14]. High speed single grain scratching test was performed using spherical tool at depth of cut ranging from 0.3  $\mu\text{m}$  to 7.5  $\mu\text{m}$  at cutting speeds of 5 m/s to 30 m/s. The results show that the higher the cutting speed, the lower the ploughing rate. Besides, the normal force during scratching is increased with the cutting speed because of the strain hardening of the workpiece while the tangential force is decreased due to reduction in the coefficient of friction between grain and workpiece [19]. Rasim et al. [12] investigated the transition of material removal phases by using a modified single grit methodology to explain interaction during the single grit and workpiece interaction. The 3D geometrical topography of the grit was analysed in terms of the parameters such as, apex angle, opening angle, rake angle, grit cutting depth and their influences on the material removal phases and chip formation were investigated. Dai et al. [21] investigated the effect of grain wear on the material removal mechanism during grinding. The diamond grains tested on the Inconel 718 material experienced four types of wear, namely, crescent depression on the rake face, abrasion on the flank face, micro fracture and macro fracture. Axinte et al. [18] and Butler et al. [20] investigated the effect of grain shaped on the material removal behaviour of ductile and brittle material. They found that the increased number of cutting edges on a single grit reduced the specific cutting force for brittle materials. For the ductile materials, reducing the contact area between the grit and workpiece is important to get a reduced specific cutting force. Klocke et al [22] developed a 2D FEM model using Deform software to simulate single grit cutting process, where the grit was 50  $\mu\text{m}$  in radius, scratching depth was 20  $\mu\text{m}$ , grit speed was 45 m/s and table speed was 180 mm/min. The simulated maximum temperature was around 1700  $^{\circ}\text{C}$ , which was within the same level with the previous analytical calculation. Using FEM, Yao et al [23] investigated the elastic contact of two dimensional rough surfaces and concluded that Hertz theory does not represent well for finer scale

geometry, where the real contact traction at the peak of an asperity would be many times higher than the results of Hertz theory. Doman et al. [24] developed a three dimensional FEM model of rubbing and ploughing phases in single-grain grinding considering elasto-plastic material characteristic. Öpöz and Chen [25] demonstrated influences of friction and depth of cut on material deformation in single grain scratching using FEM simulation in Abaqus/Standard. Recently, a 3D single grain cutting model has been developed using LS-DYNA Hydrocode [15]. In the FEM model, a hybrid formulation combined the Eulerian and Lagrangian formulation was used. The scratch profiles obtained from simulations demonstrated that the cutting mechanics changed with increasing of cutting speed due to reduction of material pile up with increasing speed. It is noted that transition between rubbing, ploughing and cutting is not clear and sometimes these actions occur simultaneously. Dai et al. [17] investigated the effect of grinding speed and undeformed chip thickness during single grit grinding of Inconel 718. They modelled a 2D single grit body with a negative rake angle ( $30^\circ$ ) and truncated base for the FEM simulation. They found a critical grinding speed (150 m/s), the effect of dynamic strain hardening and strain rate hardening are more influential if the grinding speed is lower than the critical value. Wang et al. [3] performed finite element simulation of high speed single grit grinding to investigate the transformation between material removal stages from friction sliding to ploughing, and to cutting process. They also investigated the effects of different grinding parameters and shape of abrasive grains on chip shape. Furthermore, Yiming et al. [4] investigated the grit wear and fracture and its effects on material removal mechanism by means of finite element analysis of single grit scratching simulation. The single grit body was modelled as a truncated diamond shape with a  $-30^\circ$  rake angle.

In this paper, the material removal mechanism with the single grit is investigated with computational modelling and simulation techniques including finite element method. In addition, some experimental tests under various conditions are investigated to explain material removal phenomena and surface creation during grinding.

## 2 Single grit scratching methods

### 2.1 Single grit grinding test

Using a simple single-grit test rig accommodated on the Nanoform 250 grind machine as shown in Fig. 2, the material removal was investigated by using a cubic boron nitride (CBN) grit to scratch workpiece as it acts in a grinding process. The CBN (40/50 mesh) grit size was around 0.5 mm in diameter. Two different scratching methods, traverse scratching and longitudinal scratching methods, based on a relative movement between single grit wheel and worktable were used to explore the effects of scratching methods on the material removal mechanism. In the traverse scratching method (Fig. 3-(bottom picture)) the steel wheel moves in +z direction to produce scratches with various cutting depths on the slightly tilted workpiece surface. In longitudinal scratching method (Fig. 3-(top picture)) the steel wheel moves in +x direction to produce scratches at preset depth of cut. The latter method allows investigating the effect of worktable speed on the scratch profile formation and material removal. By using these two methods, several scratches produced with changed depths and lengths depending on the grit-workpiece engagement are analysed in terms of rubbing, ploughing and cutting phenomenon. The workpiece material employed for the tests are En24T steel and En8 steel with hardness of 289.2 HV and 222.2 HV at 1 kg measuring load, respectively. Pile up ratio and actual material removal area is often used to analyses the single grit scratches in terms of ploughing and cutting behavior of the abrasive grit associated abrasive grit cutting edge shapes and micro edges. The formula of determination of pile up ratio and actual material removal area are given in Fig. 4. It must be noted that the pile up materials on both sides of scratches could sometimes be in the form of flake shape as shown in Fig. 5. In such a case, the pile up ratio calculation from top view could give a higher value than actual value, causing an inevitable error that is difficult to eliminate currently. Detailed explanation for the single grit scratching method and analysis of material removal by using pile up ratio and actual material removal area was given in a previous paper [26].

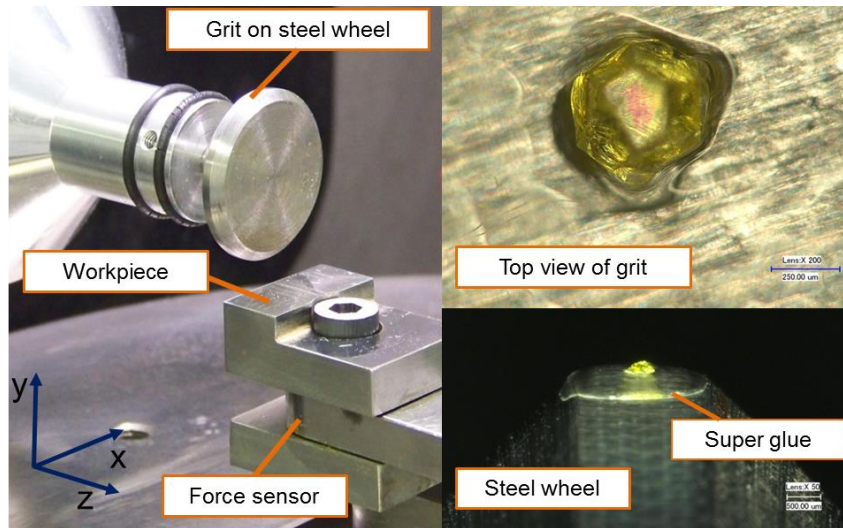


**Fig. 2** Single grit test set up on the Nanoform 250 machine

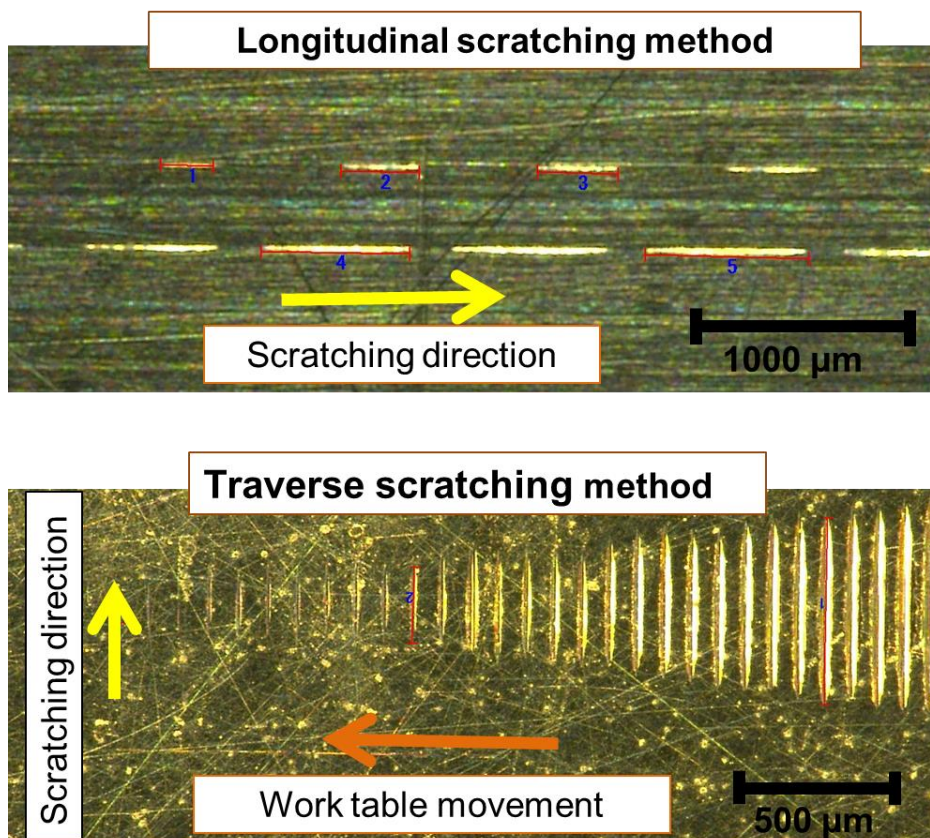


**Fig. 3** Scratches generated by longitudinal scratching method (top picture) and traverse scratching method (bottom picture)

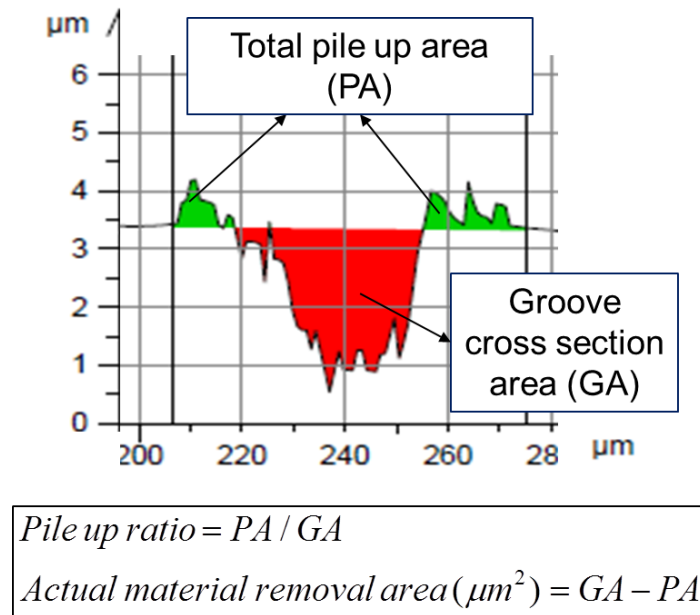


**Fig. 4** Calculation of pile up ratio and actual material removal area

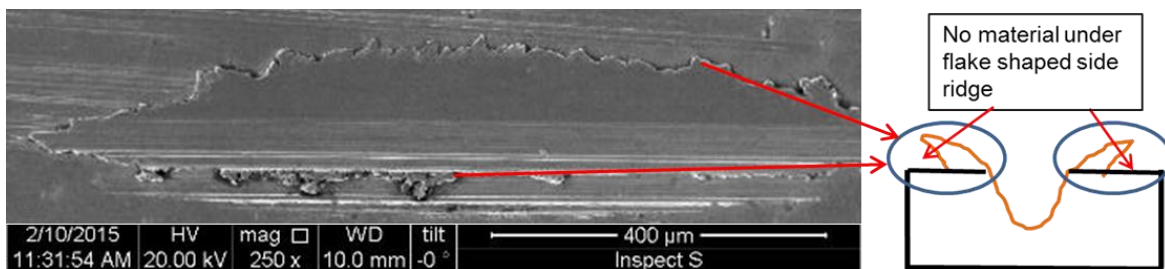


**Fig. 5** SEM image of a single grit scratch

The 3D surface topography of a CBN grit is shown in Fig. 6, which was measured before and after the traverse scratching tests by using a Keyence digital microscope. The form and colour changes in the surface topography after the tests are useful to reveal the grit wear behavior and micro cutting edge formation. In addition, continual alteration of grit cutting edges and cutting-edge apex angle was evidenced. Knowledge about the cutting edges shapes and apex angle could give a valuable insight into the modelling the single grit action on the workpiece. Macro fracture of the grit could take place during the scratching process, which created multiple cutting edges resulting in multiple edge scratches [27]. Micro fractures took place on the grit cutting edges increases the

cutting ability of the grit and improves the grit-workpiece engagement although which led to some tiny scratches within a main scratch groove [27]. These tiny scratches could play an important role in determination of final surface quality and surface finish. The wear flat on top of grit is a well-known phenomenon during grinding process that can be observed in Fig. 6(b), marked as worn edges, and some discoloration took place on the grit worn edges (wear flat) due to thermal effect caused by frictional wear between the grit and workpiece. During grinding process or single grit scratching, the abrasive grit engages with workpiece in multiple dimensions, the front edge, side edge and flank edge of the grit engaged with workpiece materials could be very difficult to define during grinding. However, some assumptions could be made to reduce the number of parameters to cope with for the analysis of the grit-workpiece interaction and resultant wear and material removal mechanism. The 2D grit profiles (Fig. 6(c)) extracted from the worn grit by using the two profile lines (*line a* and *line b*) can give an idea about the grit cutting-edge apex angle. Prevailing assumption during modelling of the single grit is a tool with negative rake angle. The grit profiles in Fig. 6(c) confirms the assumption is right but it is difficult to say what could be cutting edges engagement angle due to continual alteration of the cutting edges during the scratching and grinding process.

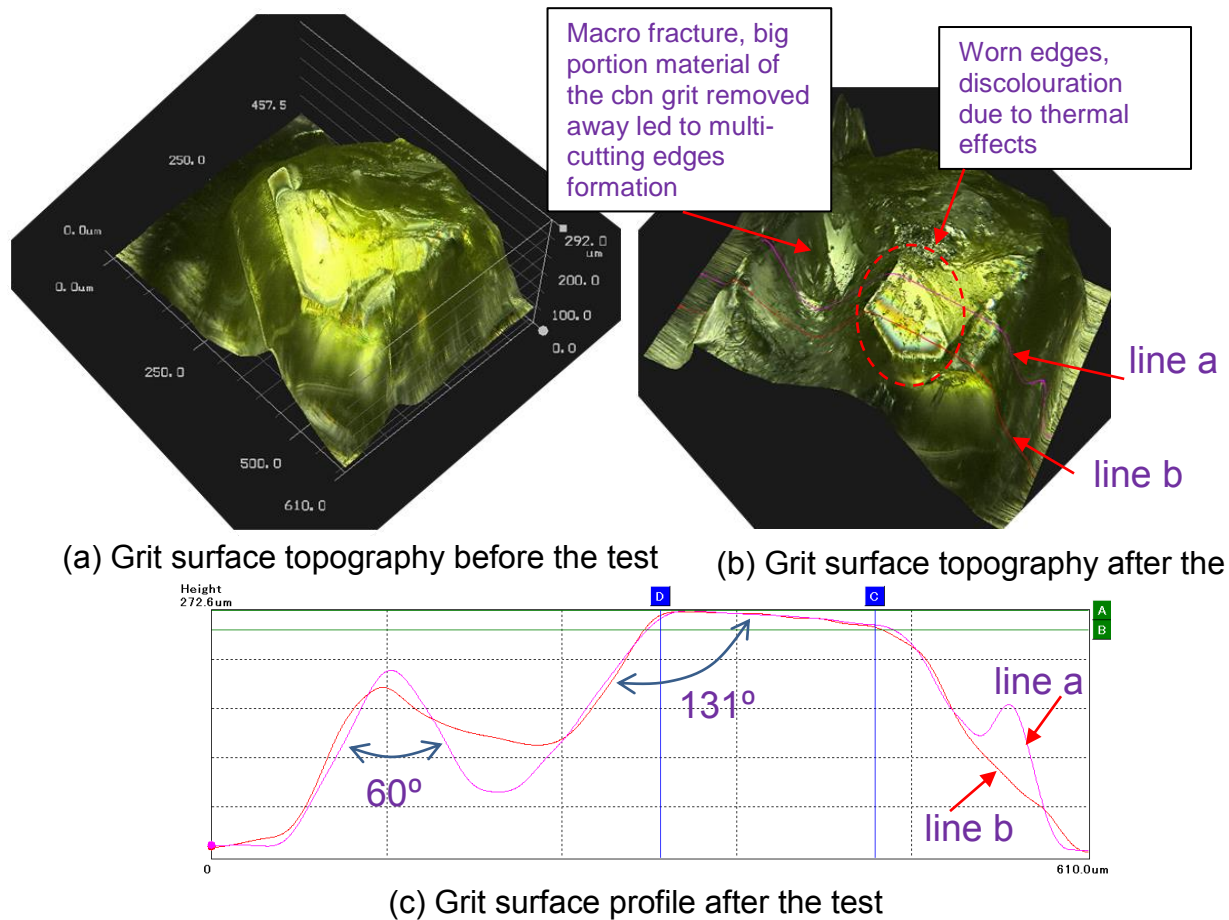


**Fig. 6** Grit surface topography (a) before single-grit grinding test, (b) after single-grit grinding test, and (c) grit surface profile measured after the single-grit grinding test

## 2.2 Finite Element Simulation to analyses the rubbing and ploughing

Material properties of grit and workpiece used in the FEM simulation are shown in Table 1. The grit is modelled as a solid semisphere with a radius of 50  $\mu\text{m}$ . Rigid body constraint set for the grit body. The length, width and depth of the workpiece are 2 mm, 1 mm and 0.5 mm respectively. The grinding path of single grain for FEM simulation is shown in Fig. 7. A range of cutting depth ( $a_{p,max}$ ) was set from 0.5  $\mu\text{m}$  to 5  $\mu\text{m}$ . In this research, the FEM simulation of a single grit scratching is conducted by using ABAQUS/standard software.

**Table 1** Material properties of the workpiece used in the finite element simulation

Material	$\rho$ (kg/ m <sup>3</sup> )	$E$ (GPa)	$\nu$	Plastic properties				
				$\sigma$ (MPa) yield stress	180	200	250	300
Workpiece	7800	200	0.3	$\epsilon$ (plastic strain)	0	0.1	0.25	0.3
Grit	Rigid body							

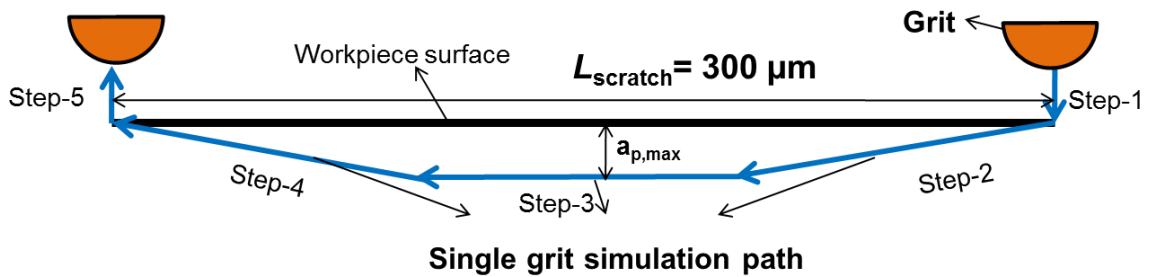


**Fig. 7** A single grit FEM simulation path

A typical mesh of the grit and workpiece is C3D4 element that is a four-node linear tetrahedron elements are used to mesh both the grit and workpiece. Free-mesh technique was used in the first stage. Coarse meshing may result in poor conformity of simulation due to the relatively large stress gradients in the grinding contact zone. In the FEM model of grinding surface creation, remeshing is used to control distortion of element due to dramatically increasing strain rate at large deformation. Fine meshes over the cutting area also provide better conformity of contact between grain and workpiece. The remeshing technique based on the refinement and coarsening techniques is applied to workpiece model to avoid entirely remeshing the workpiece. The remeshing is governed by mesh element size and average plastic strain error indicator is used to make decision about satisfaction of element geometry and contact conformity within the interaction area. Remeshing rules are needed to be defined to deal with remeshing procedures. Remeshing rules enable Abaqus/standard to adapt the

model's mesh iteratively to meet error indicator goals that have been specified. The remeshing rule has no effect on the mesh during the first simulation (Fig. 8(a)). However, during the first simulation Abaqus uses the remeshing rule to calculate the error indicator output variables. In subsequent adaptive remeshing iterations, the remeshing rule augments the mesh size specification to produce a mesh that attempts to optimize element size and placement to achieve the error indicator goals described in the rule. Workpiece remeshed with three iterations for the simulation is shown Fig. 8. Encastrate boundary conditions (all translational and rotational degree of freedom are fixed) are applied to workpiece bottom plane nodes. A two directional displacement boundary condition (-Z and -X) is applied to the nodes on the grit top flat surface to simulate indentation and sliding respectively. Boundary conditions are created in the first step and propagated through all steps. Displacement boundary conditions are modified according to the grit scratch simulation path.

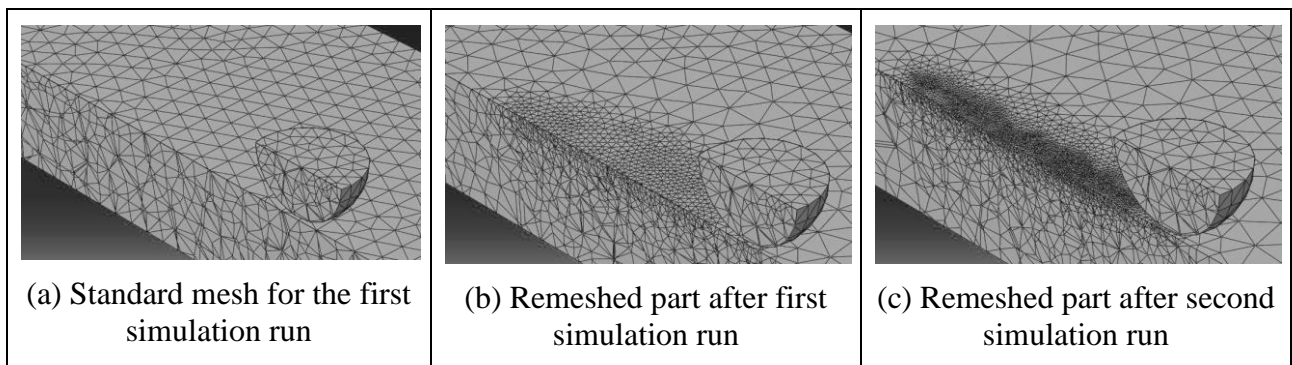


**Fig. 8** Remeshing the workpiece with iterative adaptive remeshing technique

### 3. Analysis of single grit scratch

#### 3.1 Rubbing and ploughing action along scratch path

Single grit grinding process or scratching process is normally completed with the action of rubbing, followed by ploughing and cutting phenomenon. Rubbing action does not include plastic deformation, which is merely occurred within the elastic limit of materials. It occurs at the initial stage of scratching when the grit starts to penetrate into workpiece. Within the elastic deformation

range, the grit only slide over the workpiece without generation any marks but this range is extremely small and it is difficult to measure both in experimental tests and in simulations. However, ploughing actions, including both elastic and plastic deformations, are more apparent compared to rubbing actions. Measurement of rubbing phase is quite difficult using FEM simulation. Rubbing phase is supposed to not include any plastic deformation, however, measurement from meshed element even at first contact stage have plastic strain components. In order to measure rubbing phase, it is required to make some acceptable assumptions on a measurement method. If maximum plastic strain is used as an indicator to measure the rubbing phase, contour plastic strain distribution across the simulated scratch will give some information about rubbing phase as shown in Fig. 9. The length difference between first contact point and lower level of plastic strain contour colour distribution can give approximate measurement of rubbing length. With this method, the rubbing length is measured as 5.825  $\mu\text{m}$  in the simulation of frictionless condition.

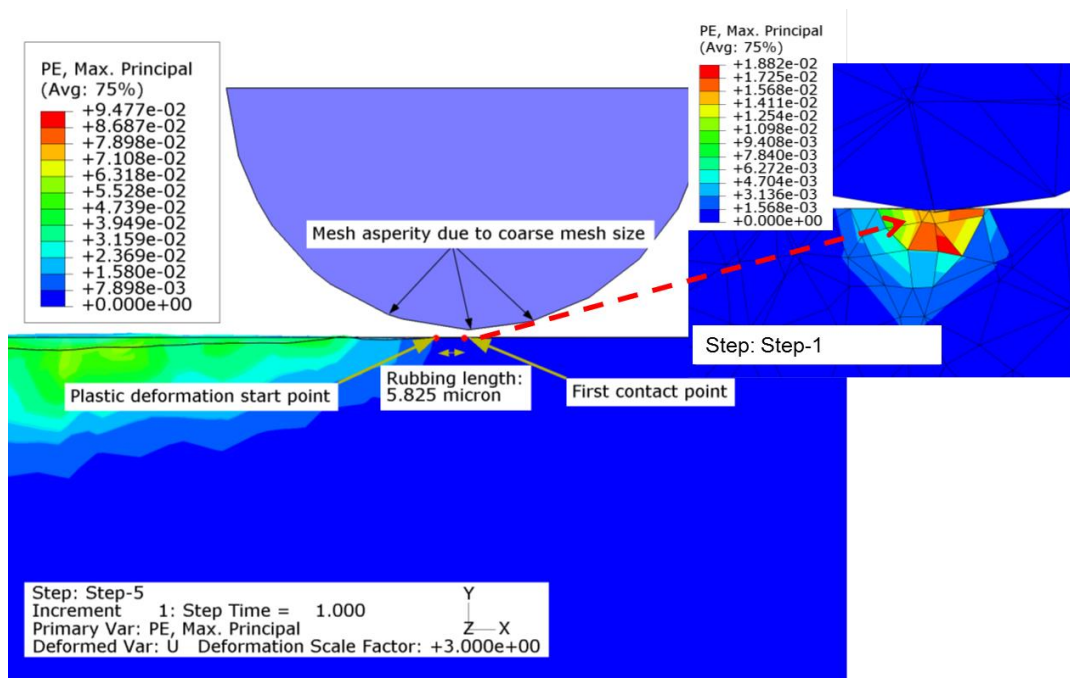


**Fig. 9** Rubbing phase using plastic strain contour as an indicator

The pile up ratio along the grit simulation path and a transection view during the single grit simulation is shown in Fig. 10, where the largest depth, at the end of step-3, includes elastic and plastic deformation. The residual deformation represents plastic deformation. Workpiece material in front of grit (front lip) is agglomerated which will lead to onset of chip formation when the stresses reach the breaking point, chips may form. Stresses due to elastic deformation are removed from the workpiece and only residuals due to plastic deformation remain on the workpiece. Pile up ratio along the grit scratching path is continuously increasing towards the end of scratch, however, there is a dramatic increase in the exit side of the scratch. Adding friction effect contributes the plastic deformation and results in greater pile up ratio. The higher the scratch depth gives the lower pile up ratio in the entrance side of the scratch, and this trend last until the grit begin to move upward in the exit of the scratch (in step-4). In the exit side of scratch (step-4), generally higher the depth of cut gives higher the pile up ratio. Pile up ratio along a real scratch (in Fig. 11) shows similar trend with the simulation result. Pile up ratio drops less than unity in the middle of scratch due to chip removal, but it increases dramatically towards the end of scratch. At the end of scratch, the pile up ratio is generally higher than 5 and even reaches up to 28, that is, a big portion of plastically deformed bulged material (ploughed lip) is agglomerated above the workpiece surface level, and the final part of scratched groove is formed within this bulged material above the original surface level. In the entrance side of the scratch, the grit was penetrating into the workpiece material, which results in compression of the work material beneath the grit body. The compression of the workpiece material could be one important reason of lower pile up ratio at the entrance side of scratch. When the grit began moving up in the exit side of scratch, it tries to uplift the work material resulting in a higher pile up ratio. The results also suggest that the cutting is the most prominent mechanism in the first half of the scratch, while the ploughing and rubbing are the dominant mechanisms in the second half of the scratch.

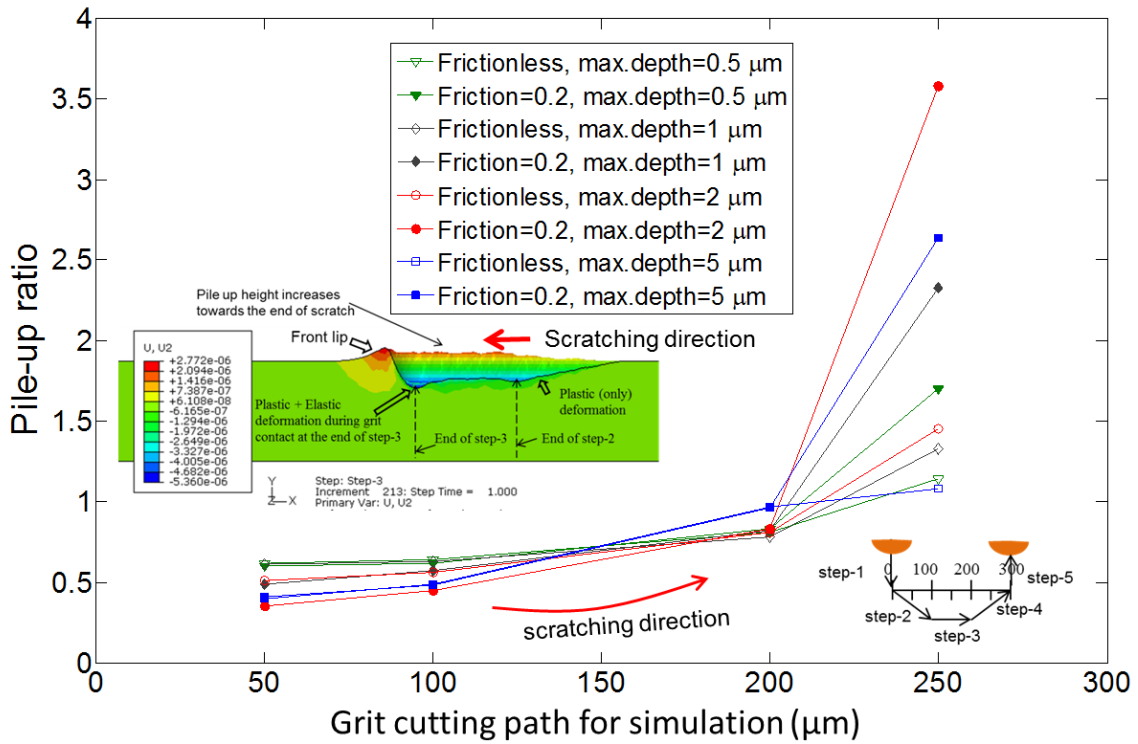


Fig. 10 Pile up ratio along grit cutting path for FEM simulation

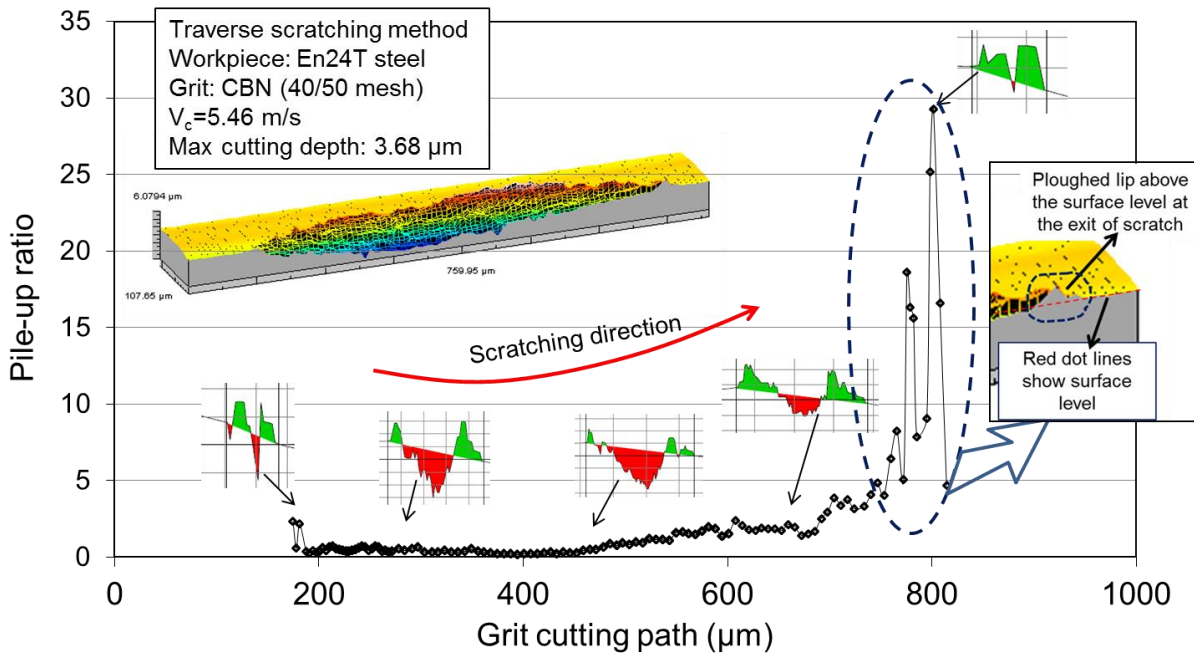
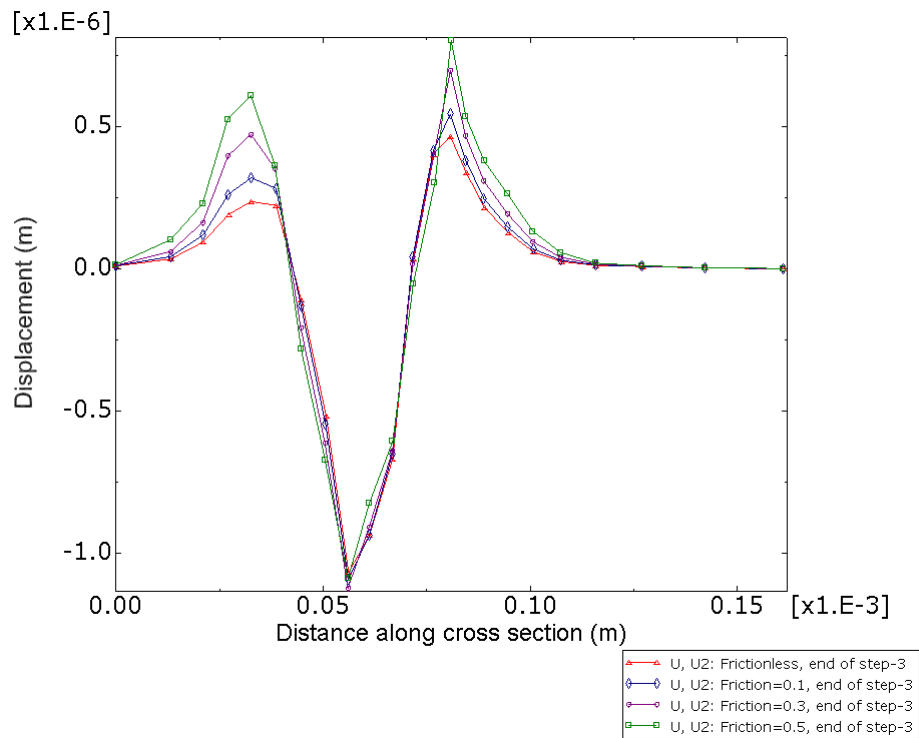
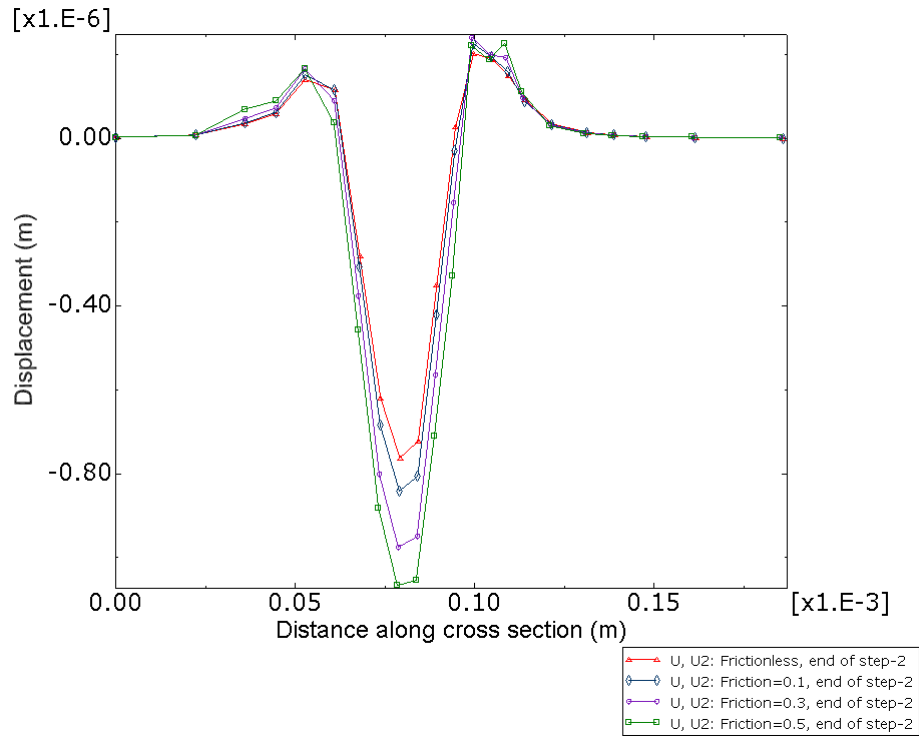
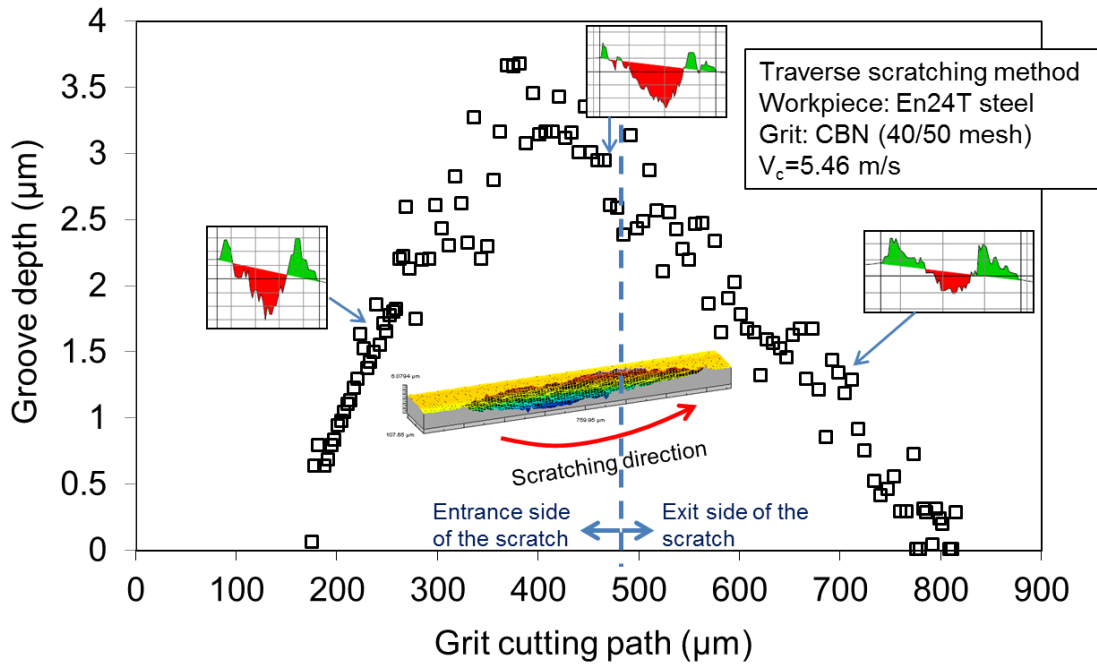


Fig. 11 Pile up ratio along grit cutting path, an experimental result

The single grit scratch path of this traverse experimental scratch shown in Fig. 11 is a circle. In the grinding that involved workpiece infeed, the cutting path is a cycloid curve. The scratch surface creation was simulated by applying the scratching path as shown in Fig. 7. A set of sectional profiles of the simulated scratches are extracted from the end of step-2 (Fig. 12-(a)) and from the end of step-3 (Fig. 12-(b)), where the maximum cutting depth ( $a_{p, \max}$ ) is 2  $\mu\text{m}$ . The gouge depths in Fig. 12-(a) become larger with increasing friction coefficient between the grit and workpiece, although, changes in the side pile up areas are not significantly different. However, the gouge depths in Fig. 12-(b) are almost constant irrespective of the friction coefficient, while the side pile up areas are significantly different and become larger with the increase of the friction coefficient. That is, plastic deformation with addition of friction coefficient become severe at the bottom side of the scratch when grit penetrates into the workpiece, and however, it is significant at the top side of scratch (in the form of pile up) when the grit is climbing up towards the end of scratch. Experimental results shown in Fig. 13 also confirm this behaviour, the transection profile of the scratch shows larger gouge depth in the first half of the scratch compared to that in the second half of the scratch.



**Fig. 12** Sectional profiles of simulated scratches with various friction coefficients



**Fig. 13** Groove depth along the grit cutting path

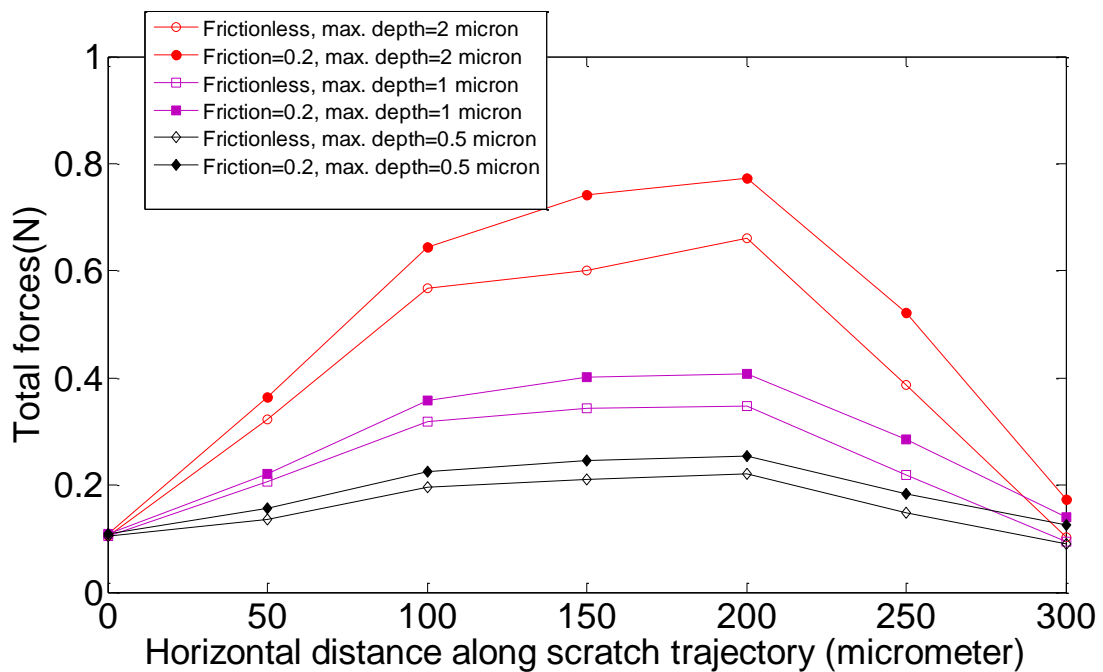
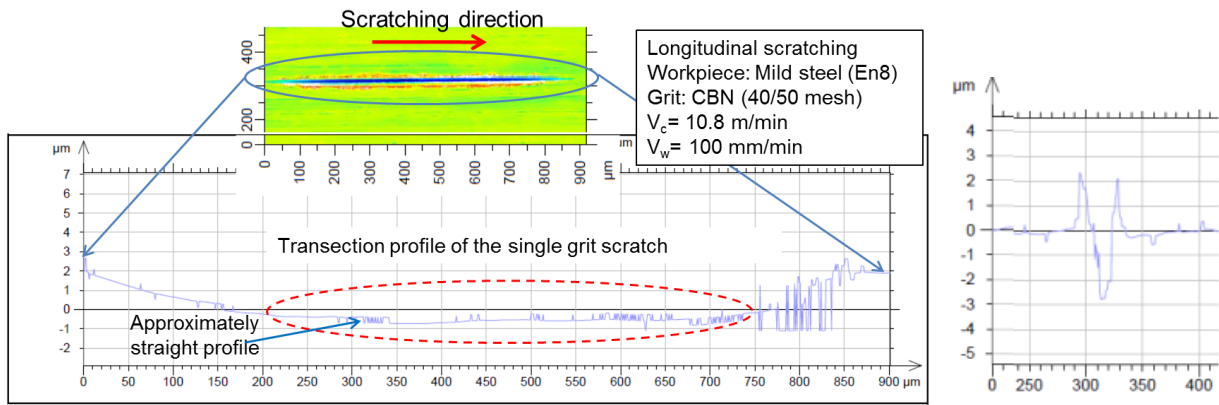


**Fig. 14** Total forces exerted by the grit during simulation

Variation in the total force along the scratch simulation path is shown in Fig. 14. Total forces increase with increase of depth of cut and friction coefficient. It increases slowly along the straight path (step-3) due to ploughed material accumulation in front of the grit.

### **3.2 Material removal analysis in longitudinal scratches**

The single grit scratching test was performed on En8 steel which has a lower hardness value (222.2 HV) than En24T steel (289.2 HV). The scratching test was performed in longitudinal direction, which is closer to real grinding process. The scratch longitudinal transection profile and scratch path section profile are shown in Fig. 15. The worktable movement and speed during scratching could affect the scratching mechanism and grit cutting path. The grit scratching path is not similar to that obtained in traverse scratching method. Middle part of the scratch path is almost straight due to the effect of work table movement in the same direction. Fig. 16 and Fig. 17 show variations in pile-up ratio against depth of cut and groove area, respectively. Cross sectional profiles for the calculation of pile up ratio and actual material removal are extracted from the middle of scratches, where the chip removal is generally more efficient. The less the depth of cut or groove area the higher the pile-up ratio. The grit cutting edge shape could be assumed in the same shape of the scratch section, thus, the scratches in Fig. 16 and Fig. 17 indicate the cutting edge is sharp. Fig. 18 shows some scratches with a truncated tip grit resulting in lower pile up ratio with lower depth of cut. These results show how the material removal is influenced by the geometrical shape of the grit cutting edge. Actual material removal is shown in Fig. 19. Up to 2.5  $\mu\text{m}$  depth, chip removal strength increases slowly with depth of cut, but when the depth of cut increases beyond the 2.5  $\mu\text{m}$ , the chip removal strength increases rapidly with depth of cut. This means that after certain depth of cut, the chip removal mechanism becomes more dominant than the ploughing mechanism.



(a)

(b)

**Fig. 15** (a) Scratch longitudinal transection profile and (b) cross sectional profile in longitudinal scratching method

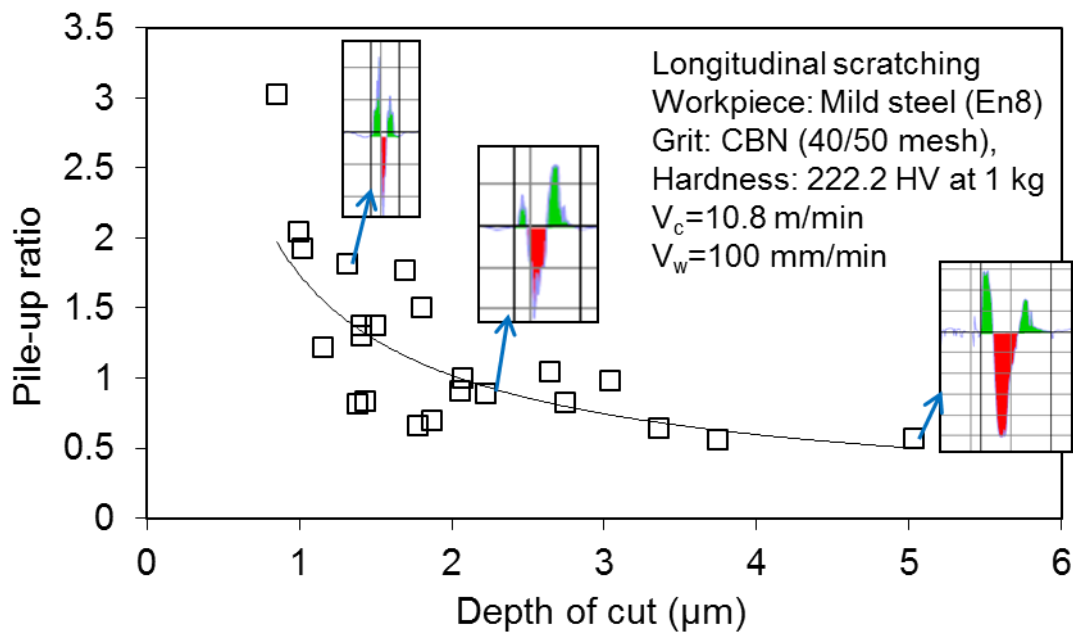


**Fig. 16** Pile up ratio versus depth of cut

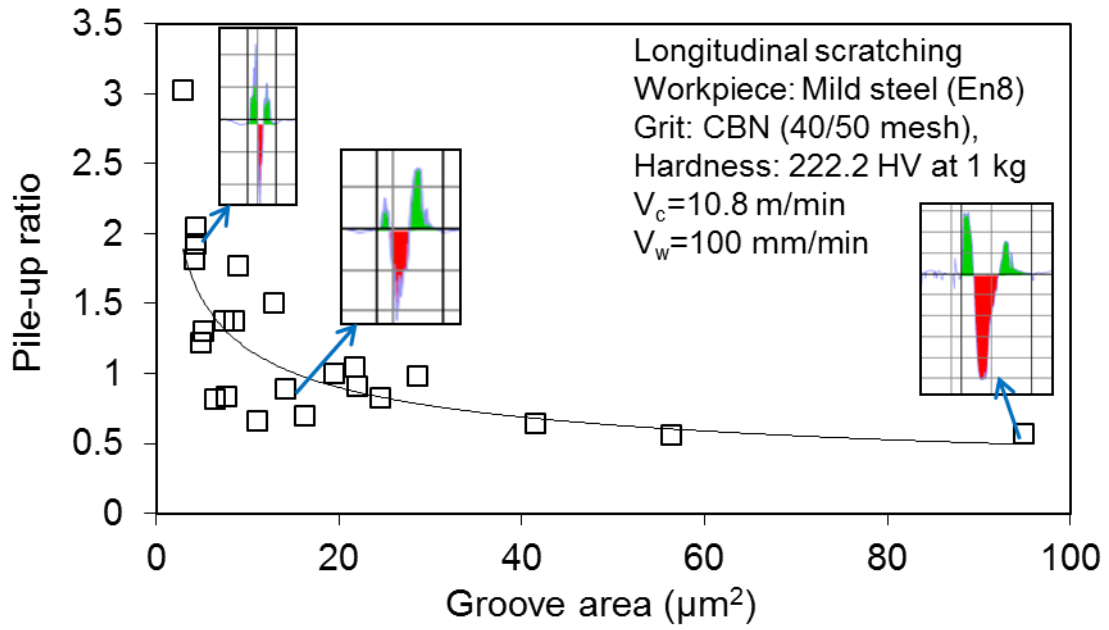


Fig. 17 Pile up ratio versus groove area

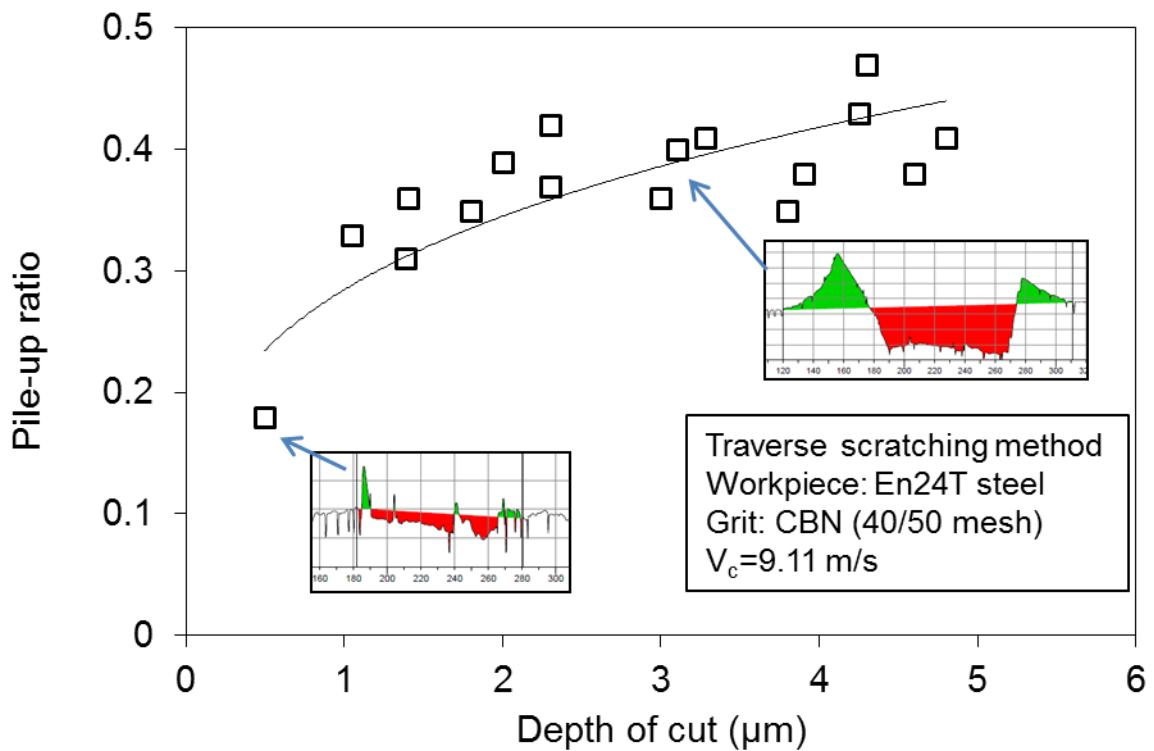
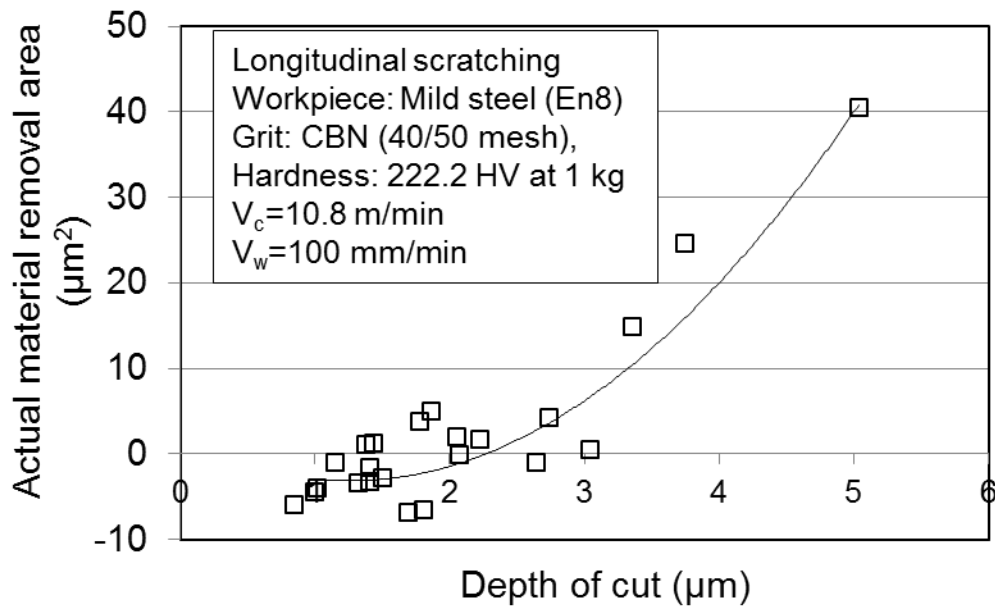


Fig. 18 Pile up ratio versus depth of cut for the grit with flat bottom



**Fig. 19** Actual material removal area versus depth of cut

### 3.3 Multi passes scratch simulation

The surface creation in grinding is achieved by a large number of grits passing through grinding zone interacting with workpiece material with rubbing, ploughing and cutting phases. In grinding, rubbing phase is elastic deformation, which does not create new surface. Ploughing is plastic deformation which pushes materials away from their original positions forming a new surface. Chip formation removes materials from workpiece due to excessive plastic deformation leaving a new surface. Because of small depth of cut, in grinding, a larger proportion of grinding actions is ploughing, which is the major factor that determines final surface features. The ploughing action of subsequent grits could alter the surface profile produced by previous grit pass. A simulation is designed to demonstrate how ploughing could affect the generation of ground surface in grinding, where a single grain scratches the workpiece three times with  $10 \mu\text{m}$  feed in transverse direction. Fig. 20 shows generated surface after three times grit scratch subsequently. Fig. 21, obtained from the end of step-3 in the grit simulation path, shows subsequent grit passes push material aside forming ridges

which alter the ground surface. Cross sectional scratch profile extracted by using a path based on element nodal locations, which are selected at the end of step-3 as shown in Fig. 20. Using the scratch profile, the pile up ratios are calculated and shown in Fig. 21. There are not any significant changes on pile up ratio with subsequent scratch formation. Both pile up area and groove area increases at every subsequent scratch, and the pile up ratios are around 0.76. However, the subsequent scratches give larger groove depth and the groove shape becomes unsymmetrical as shown in Fig. 20 and Fig. 21. Larger the depth of groove with the increase of subsequent scratch number can be attributed to the elastic-plastic deformation mechanism. Fig. 22 shows the force variation through grain simulation path for three consecutive parallel passes. Although normal forces are slightly higher in the first grain pass at step-3, there is no significant differences in normal ( $F_y$ ) and tangential ( $F_x$ ) forces for the consecutive three passes. However, increasing volume of side ploughing with the number of subsequent parallel passes leads to increase of traverse force component ( $F_z$ ) in the direction of grit traverse feed movement. Material accumulation (front ploughing) ahead of the grain when the grit advances at step-3 leads to increase of tangential forces ( $F_x$ ) in every subsequent parallel pass as shown in Fig. 22.

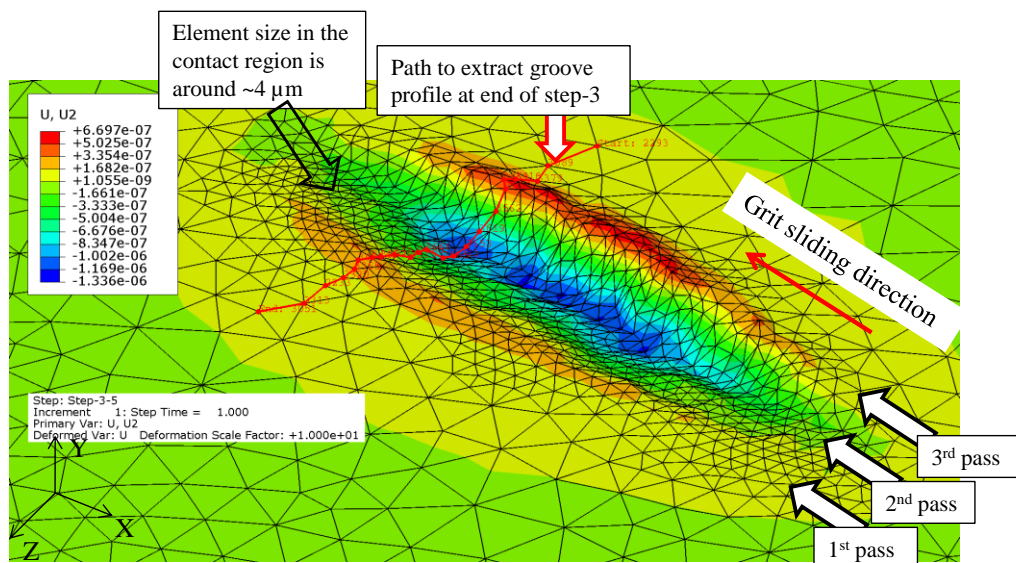


**Fig. 20** Multi-pass grit grinding simulation

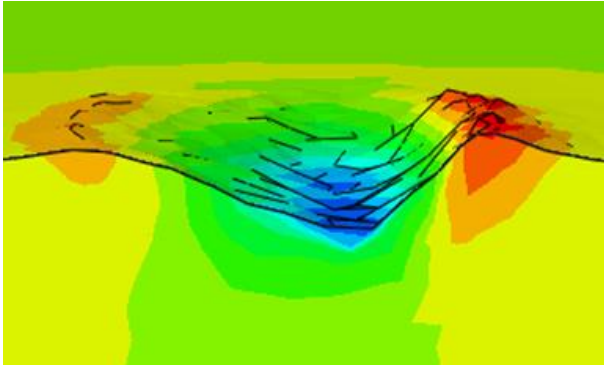
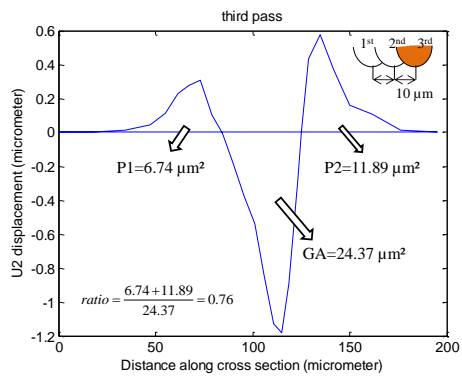
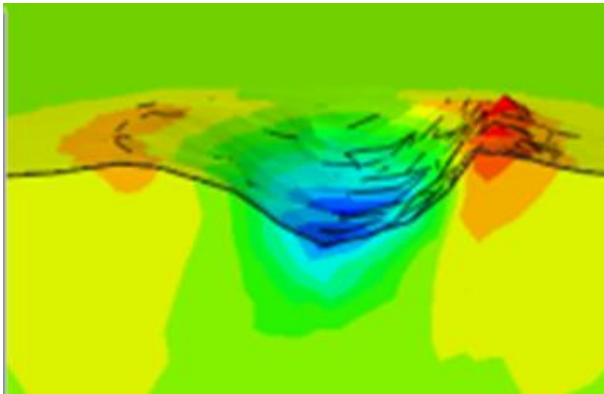
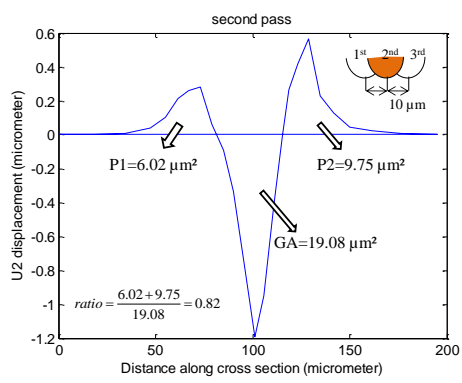
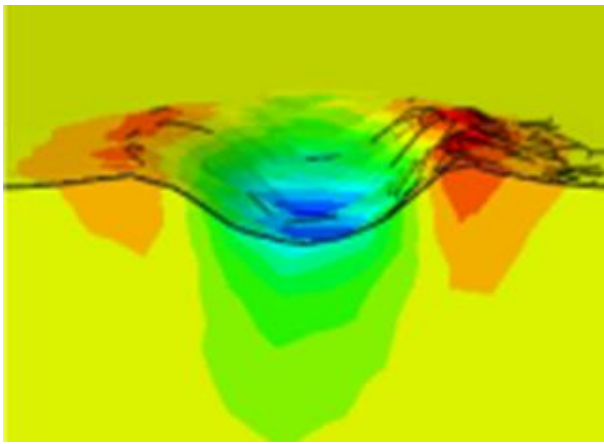
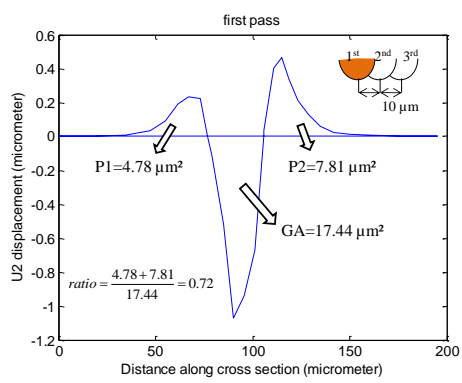
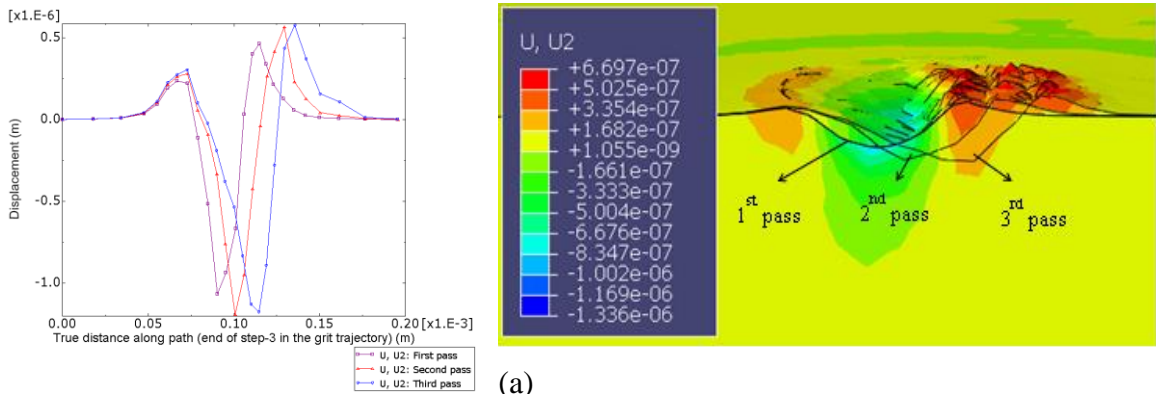


**Fig. 21** The deformation presented after 3 parallel scratch passes with 10  $\mu\text{m}$  apart

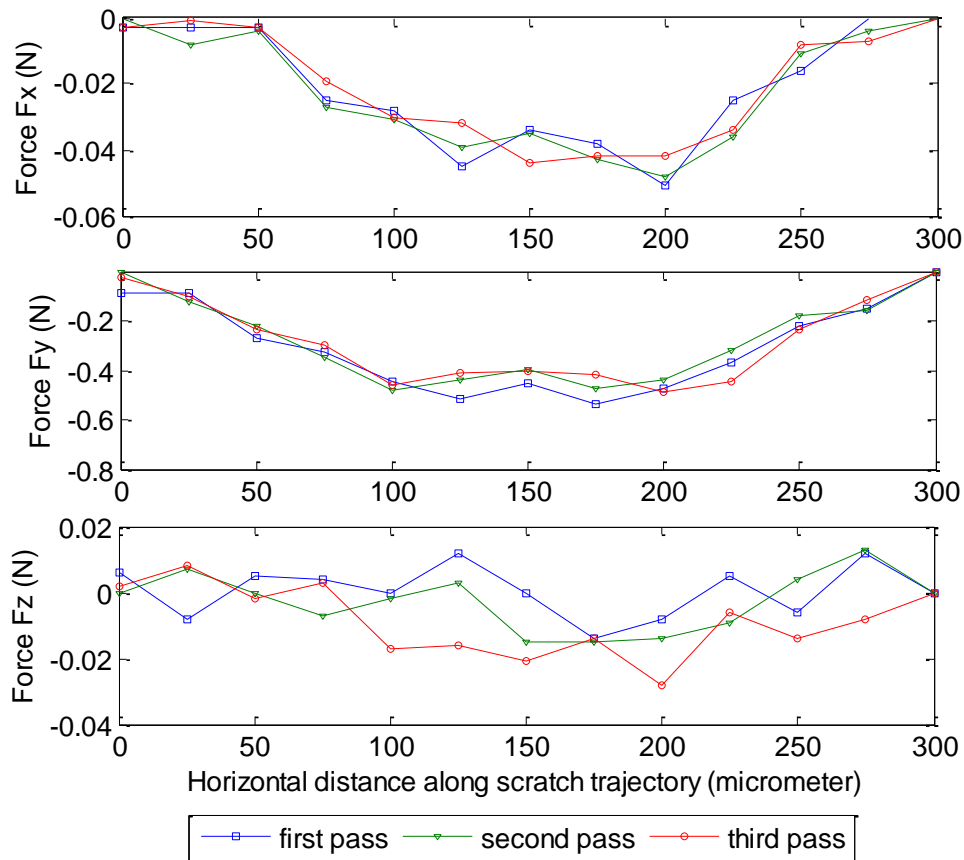


**Fig. 22** Parallel scratch force variations

#### 4 Discussion of the results

With experimental and FEM analysis, single grit scratching modelling can effectively presents the basic grinding material removal mechanism, namely rubbing, ploughing and cutting. Associated with ground surface formation, the grinding-induced forces and stresses can be investigated by varying different process conditions at different scale levels. Using a commercial software package of ABAQUS/Standard, the rubbing and ploughing phenomena of single grit scratching has been successfully illustrated similar to that in real experiments. Experimental and numerical results suggest that three prevailing phases of grinding material removal is occurring simultaneously during the grit-workpiece interaction. However, the weight of these phases could be different and alter depending on

the position and location of the grit over the scratching path. Further, the grit geometry, grinding pass sequence (longitudinal or traverse), grit engagement depth, grit wear due to fracture and attrition, as well as workpiece material properties (brittle or ductile) are all influential to the weight of each phase. Rubbing phases can only be approximately estimated as shown in Fig. 9 in the FEM model, even it is more difficult to estimate the rubbing length with the experiment. Anderson et al. [15] also indicated that no clear transition from rubbing to ploughing to cutting could be identified in their experimental and numerical investigation. By attaching a grit on the worktable and fixing the workpiece on a rotational wheel, Rasim et al. [12] used a modified single grit scratching test to observe the material removal phases. This modified test provided slightly better observation of rubbing and chip formation phase, however, their results were also acquired by some sorts of approximation. Their finding suggests that the rubbing phase generally occur at the grit entrance to the workpiece and the grit exit side of the scratch mostly deformed by plastic deformation, which is supportively agreed with the result given in Fig. 11. Ploughed lip above the work surface level at the exit side of the scratch demonstrated that the dominant mechanism is the ploughing. The cutting mechanism where the actual chip removal occurs is the more effective mechanism in the first half to the scratch, which is obvious in Fig. 11, where the lower pile up ratio in that region suggest this fact. Although the material removal mechanism affected by the workpiece material mechanical property, similar trend was found with Inconel 718 workpiece material in [27]. FEM simulation results in Fig 12 also support the experiments, friction only affects the grit gouge depth in the first half of the scratch, whereas material pile up on the both sides of the scratches are increasing with addition of friction coefficient while the grit gouge depth is stable.

The grit geometry of cutting edges is one of the most influential parameters that could alter the material removal mechanism significantly. A single cutting edge with a pyramid shape as shown in Fig. 16, often considered as a sharp edge, has a higher pile up ratio with lower depth of cut; contrary to Fig.16, a truncated cutting edge shown in Fig. 18 would have a higher pile up ratio with increasing depth of cut. Such a contradictive behaviour of grit scratch requires a thorough investigation of the

influence of grit cutting edge geometry on grinding material removal mechanism. It is critically important, especially, for an engineered grinding tool designed with shaped abrasive grains in a certain arrangement [18]. FEM analysis method presented in this paper is proved to be a powerful to illustrate single grit grinding performance with irregular abrasive grains. For a reliable FEM modelling, the re-meshing strategy is critical to provide very fine size meshes in contact area to alleviate the element distortion due to large plastic deformation. The FEM simulation provides essential information of grinding performance, including stress distribution and surface formation during grinding. Further, ploughing ridge formation, rubbing deformation and material removal characteristics can also be studied. However, the cutting phenomenon is still difficult to fulfil at submicron or nanometre level because of the extremely high distortion within grinding zone under high negative rake angle of the grain, which significantly increase the demand of computing resource. Therefore, molecular dynamics method was introduced for the study of surface creation at nanometre level [6, 28, 29]. However, the computing power and simulation time could also be an obstacle for its application due to the number of molecules involved.

## **5 Conclusions**

With the support of experiments and FEM analyses, some key findings are summarised below.

- Single grit grinding material removal process consists of rubbing, ploughing and cutting three stages, through the transition between these stages could not be clearly cut. The ploughing performance in grinding has significant influence on the ground surface creation.
- Pile up materials is significantly increases towards the end of grit scratch due to material accumulation in front of the grit while the grit advances towards the scratch exit. During the grit climbs up towards the exit end of the scratch, the uplifted agglomerated materials will stay on the surface, leading to a high pile up ratio at the end of the scratch.

- The grinding force variation depends on the cutting path of the grit. The bulged material due to previous ploughing action will increase the cutting forces in subsequent cutting passes.
- Friction between the grit and workpiece has notable contribution to plastic deformation, resulting in larger penetration depth in the entrance stage of the scratch and higher bulged material ridges and pile up along the scratch pathway.
- Side pile up increases in a grit multi pass simulation in the direction of grit cross feed movement, the normal force ( $F_y$ ) is the larger in the first pass of multi pass simulation, however, tangential forces ( $F_x$ ) are quite stable.
- In longitudinal scratching test, the middle of grit cutting path took a rather flat profile due the worktable movement ( $V_w$ ), which is consistent with the grit path in the FEM model. The agglomerate materials at the front of the grit will accumulated leading to a decrease of real depth of cut, even the undeformed depth of cut remain the same. As a result, the actual gouge depth in the penetrate side of the scratch becomes larger than that in the exit side of the scratch
- A sharp grit will give higher pile up ratio than a blunt grit. However, when the cutting depth increases, the pile up ratio will decrease for the sharp grit and will increase for the blunt grit. This finding could provide an important guidance for grinding wheel design to improve grinding efficiency.

## References

- [1] Brinksmeier, E., Aurich, J. C., Govekar, E., Heinzl, C., Hoffmeister, H. V., Klocke, F., Peters, J., Rentsch, D., Stephenson, D. J., Ulmann, E., Weinert, K., and Wittmann, M., 2006, "Advances in Modeling and Simulation of Grinding Processes," *CIRP Annals-Manufacturing Technology*, 55(2), pp. 667-696.
- [2] Doman, D. A., Warkentin, A., and Bauer, R., 2009, "Finite element modeling approaches in grinding," *International Journal of Machine Tools and Manufacture*, 49(2), pp. 109-116.
- [3] Wang, L., Tian, X., Lu, Q., and Li, Y., 2017, "Material Removal Characteristics of 20CrMnTi Steel in Single Grit Cutting," *Materials and Manufacturing Processes*, 113, pp. 49-58.

- [4] Yiming, M., Zhonghua, Y., and Zhensheng, Y., 2016, "Numerical investigation of the evolution of grit fracture and its impact on cutting performance in single grit grinding," *The International Journal of Advanced Manufacturing Technology*, 89(9), pp. 3271-3284.
- [5] Öpöz, T. T., and Chen, X., 2010, "An Investigation of the Rubbing and Ploughing in Single Grain Grinding using Finite Element Method," 8th International Conference on Manufacturing Research, Durham, UK, pp. 256-261.
- [6] Chen, X., Öpöz, T. T., and Oluwajobi, A., 2012, "Grinding Surface Creation Simulation Using Finite Element Method and Molecular Dynamics," *Advanced Materials Research*, 500, pp. 314-319.
- [7] Klocke, F., 2003, "Modelling and simulation of grinding process," 1st European Conference on Grinding, Aachen, Germany.
- [8] Hahn, R. S., 1962, "On the nature of the grinding process," *Proc. Proceedings of the 3rd International Machine Tool Design & Research Conference*, Pergamon Press, Manchester, pp. 129-154.
- [9] Chen, X., and Öpöz, T. T., 2016, "Effect of different parameters on grinding efficiency and its monitoring by acoustic emission," *Production & Manufacturing Research*, 4(1), pp. 190-208.
- [10] Malkin, S., 2008, *Grinding technology*, Industrial Press.
- [11] Klocke, F., 2009, *Manufacturing Processes 2— Grinding, Honing, Lapping*, Springer-Verlag Berlin Heidelberg.
- [12] Rasim, M., Mattfeld, P., and Klocke, F., 2015, "Analysis of the grain shape influence on the chip formation in grinding," *Journal of Materials Processing Technology*, 226, pp. 60-68.
- [13] Takenaka, N., 1966, "A study on the grinding action by single grit," *Ann. CIRP*, 13, pp. 183-190.
- [14] Ghosh, S., Chattopadhyay, A. B., and Paul, S., 2010, "Study of grinding mechanics by single grit grinding test," *International Journal of Precision Technology*, 1(3), pp. 356-367.
- [15] Anderson, D., Warkentin, A., and Bauer, R., 2011, "Experimental and numerical investigations of single abrasive-grain cutting," *International Journal of Machine Tools and Manufacture*, 51, pp. 898-910.
- [16] Singh, V., Durgumanhanti, U. S. P., Rao, P.V., and Ghosh, S., 2011, "Specific ploughing energy model using single grit scratch test," *International Journal of Abrasive Technology*, 4(2), pp. 156-173.
- [17] Dai, J., Ding, W., Zhang, L., Xu, J., and Su, H., 2015, "Understanding the effects of grinding speed and undeformed chip thickness on the chip formation in high-speed grinding," *The International Journal of Advanced Manufacturing Technology*, 81(5-8), pp. 995-1005.
- [18] Axinte, D., Butler-Smith, P., Akgun, C., and Kolluru, K., 2013, "On the influence of single grit micro-geometry on grinding behavior of ductile and brittle materials," *International Journal of Machine Tools and Manufacture*, 74, pp. 12-18.
- [19] Anderson, D., Warkentin, A., and Bauer, R., 2011, "Novel Experimental Method to Determine the Cutting Effectiveness of Grinding Grits," *Experimental mechanics*, 51(9), pp. 1535-1543.
- [20] Butler-Smith, P., Axinte, D., Daine, M., and Kong, M. C., 2014, "Mechanisms of surface response to overlapped abrasive grits of controlled shapes and positions: An analysis of ductile and brittle materials," *CIRP Annals-Manufacturing Technology*, 63(1), pp. 321-324.
- [21] Dai, C., Ding, W., Xu, J., Fu, Y., and Yu, T., 2017, "Influence of grain wear on material removal behavior during grinding nickel-based superalloy with a single diamond grain," *International Journal of Machine Tools and Manufacture*, 113, pp. 49-58.

- [22] Klocke, F., Beck, T., Hoppe, S., Krieg, T., Muller, N., Nothe, T., Raedt, H. V., and Sweeney, K., 2002, "Examples of FEM application in manufacturing technology," *Journal of Materials Processing Technology*, 120(1-3), pp. 450-457.
- [23] Yao, Y., Schlesinger, M., and Drake, G. W., 2004, "A multiscale finite element method for solving rough surface elastic contact problems," *Canadian Journal of Physics*, 82(1), pp. 679-699.
- [24] Doman, D. A., Bauer, R., and Warkentin, A., 2009, "Experimentally validated finite element model of the rubbing and ploughing phases in scratch tests," *Proceedings of the Institution of Mechanical Engineers, Part B: Journal of Engineering Manufacture*, 223(12), pp. 1519-1527.
- [25] Öpöz, T. T., and Chen, X., 2011, "Single grit grinding simulation by using finite element analysis," *Proc. AIP Conference Proceedings*, AIP, pp. 1467-1472.
- [26] Öpöz, T. T., and Chen, X., 2012, "Experimental investigation of material removal mechanism in single grit grinding," *International Journal of Machine Tools and Manufacture*, 63, pp. 32-40.
- [27] Öpöz, T. T., and Chen, X., 2015, "Experimental study on single grit grinding of Inconel 718," *Proceedings of the Institution of Mechanical Engineers, Part B: Journal of Engineering Manufacture*, 229(5), pp. 713-726.
- [28] Oluwajobi, A., and Chen, X., 2013, "Effects of interatomic potentials on the determination of the minimum depth of cut in nanomachining," *International Journal of Abrasive Technology*, 6(1), pp. 16-39.
- [29] Oluwajobi, A., and Chen, X., 2017, "Molecular Dynamics (MD) Simulation of Multi-pass Nanometric Machining—The Effect of Machining Conditions," *Current Nanoscience*, 13(1), pp. 21-30.